

Determination of the bowing parameter of the split-off band in $\text{Cd}_{0.8}\text{Zn}_{0.2}\text{Te}(100)$ by angle-resolved photoemission spectroscopy

David W. Niles

National Renewable Energy Laboratory, 1617 Cole Boulevard, Golden, Colorado 80401-3393

Hartmut Höchst

Synchrotron Radiation Center, University of Wisconsin-Madison, 3731 Schneider Drive, Stoughton, Wisconsin 53589-3097

(Received 26 December 1991)

Angle-resolved photoemission spectroscopy is used to measure the width $\Omega_{s.o.} = \Gamma_7 - X_6$ of the split-off valence band in $\text{Cd}_{0.8}\text{Zn}_{0.2}\text{Te}(100)$. We find an increase in the alloy bandwidth which is ~ 2 times larger than the value expected from a linear alloy model (Vegard's rule). Using CdTe as a reference material, we determined a bowing parameter $b_p \sim 0.65$ eV for the split-off-band width in $\text{Cd}_{1-x}\text{Zn}_x\text{Te}$ alloys. The virtual-crystal approximation (VCA) works well for the upper valence bands but fails to describe the more localized d states. Chemical differences and the size mismatch between Cd and Zn atoms lead to pronounced deviations from the VCA behavior. The appearance of distinctly split Cd $4d$ - and Zn $3d$ -band emissions which we observe is outside the scope of the VCA, lending support to more sophisticated structural models which incorporate disparate Cd and Zn atoms for binary semiconducting alloys.

I. INTRODUCTION

Many electronic properties of semiconducting binary alloys can in a first approximation be assumed to be linearly related to the concentration variation in the alloy. The optical band gap is an example. However, it is frequently found that while the linear model (Vegard's rule) may describe the change in lattice constant in alloy semiconductors perfectly, it fails to explain the alloy band structure.¹ A simple theoretical model, the virtual-crystal approximation (VCA),² which replaces the individual alloy atoms (or molecules in the case of a compound alloy) with an average atom placed in the symmetry of the crystal can describe many of the observed nonlinear alloy effects much better.³⁻⁸

The VCA may produce nonlinearities in the binary alloy properties because the band structure is not linear with the crystal potential matrix elements. The model simply states that the properties $P(x)$ of an alloy of form $A_{1-x}B_xC$, where A and B are anions and C is the common cation, can be described by the equation

$$P(x) = (1-x)P_{AC} + xP_{BC} + b_p x(1-x),$$

where P_{AC} and P_{BC} represent the properties of the individual alloy components. The nonlinearities are accounted for in the VCA by introducing a bowing parameter b_p . In the absence of nonlinear effects ($b_p = 0$) the VCA is equivalent to Vegard's rule.

The VCA was appropriate in describing the major part of the bowing effect observed in the optical band gap of many isovalent alloys such as $\text{Cd}_{1-x}\text{Hg}_x\text{Te}$,⁷ $\text{ZnSe}_{1-x}\text{Te}_x$,⁹ $\text{Zn}_{1-x}\text{Cd}_x\text{S}$,¹⁰ and $\text{Hg}_{1-x}\text{Zn}_x\text{Te}$.¹¹ Wei and Zunger⁸ pointed out that in those cases where the simple VCA model failed, the alloy constituents not only had a large chemical mismatch but also showed a

significant size mismatch between the substituted cations. The effect of the structural misfit can be very pronounced and may lead to a bowing which significantly overshoots the values expected from VCA-based calculations.

The mismatch in bond lengths in addition to the chemical disparity between the cations in the binary $\text{Cd}_{1-x}\text{Zn}_x\text{Te}$ alloys generates departures from the VCA. A given Te atom may be surrounded by any combination of Cd and Zn atoms, yielding a Te-site symmetry of T_d , C_{3v} , or D_{2d} . A key ingredient is that a lowering of site symmetry leads to splittings of otherwise degenerate energy levels. In addition to the lowering of symmetry, the individual bonds are under considerable strain from the aggregate, and this strain may accentuate splittings. Results on $\text{Al}_x\text{Ga}_{1-x}\text{As}$ and $\text{Hg}_{0.5}\text{Cd}_{0.5}\text{Te}$ alloys where the size mismatch is negligible have shown deviations from the predictions of the VCA, and provided experimental support for a refined structural model.^{12,13} Alloys of $\text{Cd}_{1-x}\text{Zn}_x\text{Te}$, however, are size mismatched, since the Cd-Te bonds in CdTe are $\sim 6.4\%$ longer than Zn-Te bonds in ZnTe. The size mismatch may act as a perturbation which contributes to non-VCA behavior in the electronic structure of $\text{Cd}_{1-x}\text{Zn}_x\text{Te}$ alloys.

This paper reports experiments to determine the alloy effects in the electronic valence-band structure of $\text{Cd}_{0.8}\text{Zn}_{0.2}\text{Te}$. We investigate the valence-band dispersion $E(k)$ from the center of the Brillouin zone along the Δ direction to the X point by angle-resolved photoemission spectroscopy (ARPES) with synchrotron radiation. By comparison of the alloy data with ARPES spectra of CdTe(100), we find that the valence-band structure of $\text{Cd}_{1-x}\text{Zn}_x\text{Te}$ alloys does not follow the simple linear composition relation (Vegard's rule) which works extremely well for the lattice constant of these alloys. Rather, the experimental band mapping shows a very pronounced nonlinear effect in the width of the split-off valence band with a bowing parameter of $b_p = 0.65$ eV.

The persistence of distinct Cd 4*d* and Zn 3*d* emission features rather than an "averaged" *d*-band emission, however, indicates a limitation of the VCA. While the VCA works reasonably well to describe alloy properties of extended states it has shortcomings in predicting the alloy properties of more localized states.

II. EXPERIMENT

A Cd_{0.8}Zn_{0.2}Te single crystal was oriented along the [100] direction. The sample dimensions were 10×10×1 mm.³ The crystal was mechanically polished and chemically etched before insertion into the vacuum system. Sputtering the sample for several hours with Ar ions of 1-keV energy, followed by annealing to 300°C to remove surface contamination and the sputter damage, resulted in clean surfaces. The cleaning and annealing cycles were repeated several times until the structural quality of the sample surface, as measured by reflection high-energy electron diffraction (RHEED), did not improve further.

Figure 1 shows a horizontal intensity profile taken from a RHEED pattern along the (100) azimuth of the Cd_{0.8}Zn_{0.2}Te sample. For comparison we also show the RHEED pattern from CdTe(100) taken under similar experimental conditions. The incident electron beam energy was $E_0 \sim 20$ keV. The angle of incidence was $\sim 2^\circ$ along the (110) azimuth. One can see from Fig. 1 that the

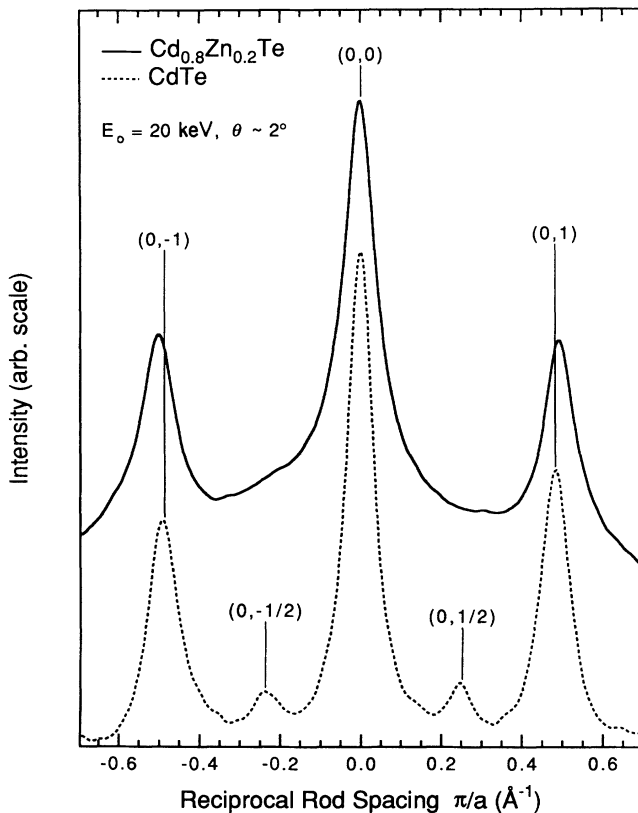


FIG. 1. Horizontal intensity profile of the RHEED pattern from Cd_{0.8}Zn_{0.2}Te(100) and CdTe(100) surfaces. The incident electron beam was 20 keV, at a 2° angle of incidence.

alloy sample does not show the half order streaks which are well developed in the CdTe sample. The lack of surface reconstruction may be a result of the natural disorder in the alloy, as well as the increase in step density, since the Cd_{0.8}Zn_{0.2}Te sample also has an increased widths of the diffracted beams compared to that of single phase CdTe.

The angle-resolved photoemission experiments were performed at the University of Wisconsin's 1-GeV electron storage ring Aladdin on the Seya-Namioka beamline. The photon energy of this beamline ranges from $h\nu \sim 10$ to 35 eV. The angle of incidence of the photons was 60° with respect to the surface normal of the sample. With this geometry, the predominant component of the electric-field vector points along the sample normal. The electric field of the photon belongs to the Γ_{15} representation at the Γ point, the Δ_1 representation for dispersion along the Δ line, and the X_3 representation at the X point.^{14,15} As we will explain later in the text, the different representations are important since they are responsible for the accentuation of emission from the split-off band at the expense of the two upper valence bands.

With the chosen monochromator entrance and exit slit settings, the resolution of the beamline was $\Delta E_{\text{mono}} \sim (10^{-4} \text{ eV}^{-1})E^2$. The minimum resolution of the monochromator was < 90 meV. The energy resolution of the electron analyzer was $\Delta E_{\text{electr}} \sim 0.15$ eV. Since the analyzer resolution is considerably less than that of the monochromator, the combined resolution of the system is practically limited by the resolution of the electron analyzer.

The resolution in k space is determined by the acceptance cone of the analyzer and the kinetic energy of the photoelectrons. Taking the acceptance to be a cone of half angle $\theta = 1.5^\circ$ gives a k -space resolution $\Delta k / G_0 \sim 6 \times 10^{-4} (E_k)^{1/2}$, where E_k is the kinetic energy of the photoemitted electron, $G_0 = 2\pi/a$, and $a \sim 6.4$ Å. The resolution for these experiments was better than $\Delta k / k_{\Gamma X} \leq 5\%$ of the width of the Brillouin zone.

III. RESULTS AND DISCUSSION

Figure 2 shows selected normal-emission spectra for photon energies in the range $h\nu = 13$ to 34.5 eV. The binding energy is referenced to the Fermi level ($E_F = 0$), which was determined from a thin metal film evaporated on the sample. The binding energy window shown in Fig. 2 covers the dispersion of the two upper valence bands and the split-off band. The valence band derived from the Te 5*s* orbital and the Cd and Zn *d* states is at higher binding energy. These states will be discussed later.

The prominent photoemission feature which disperses from $E_b \sim 1.9$ eV at $h\nu = 15.0$ eV to $E_b \sim 5.4$ eV at $h\nu = 34.5$ eV results from transitions from the split-off valence band into segments of three distinct final-state bands.^{15,16} The first final-state band covers the range $h\nu = 15.0$ to 18.5 eV; the second band picks up at $h\nu = 18.5$ eV and continues to $h\nu = 24.5$ eV, and the third band goes up to $h\nu = 34.5$ eV. One may see the contributions of the individual final-state bands in the

spectra measured at $h\nu=18.5$ and 24.5 eV, where small but noticeable shoulders appear at lower binding energies. A more thorough analysis of final-state bands in zinc-blende semiconductors has been given elsewhere.¹⁵

The three final-state bands may be approximated with one free-electron-like band.^{15,16} In the simple model where the final-state bands are assumed to be free-electron-like bands, the energy of the primary cone final state band is given by

$$E_k = \hbar^2(\mathbf{k} - \mathbf{G})^2 / (8\pi^2 m) - U_0,$$

where U_0 is the inner potential measured from the valence-band maximum (VBM) and \mathbf{G} is a reciprocal-lattice vector normal to the (100) surface.^{17,18} For the transitions into this band, we found the reciprocal vector $|\mathbf{G}_{200}| = 2\pi/a$ and inner potential of $U_0 = 4.25$ eV gave the best agreement between experimental data and known valence-band structure.

As the photon energy increases, the split-off band transition disperses and merges with a density-of-states (DOS) feature at $E_b \sim 5.4$ eV which is present in all of the spectra. The DOS feature results from the flat portions of the valence bands near the X_6 point. At $h\nu = 34.5$ eV, the DOS and split-off band transitions coincide, meaning that the direct transition reaches the X_6 point at the end of the Brillouin zone. One can also see from the $h\nu = 14$

and 15 eV spectra that the split-off band transition starts at the Γ point around $h\nu \sim 15.0$ eV. The spectral range of $h\nu = 15.0$ to 34.5 eV thus maps the dispersion of the split-off band from Γ_7 to X_6 . Since the critical point energies of this band are well marked by the additional DOS features the bandwidth of the split-off band may in principle be determined without making any detailed assumptions about the final-state bands.

It is noticeable from the spectra that emission from the upper two valence bands is very weak. For $h\nu = 14$ eV, one sees emission from Γ_8 at $E_b \sim 1.0$ eV. Increasing the photon energy forces the transition to occur along the Δ line. The symmetries of these two bands are predominantly Δ_3 and Δ_4 (representations without electron spin). Since the dipole operator responsible for these transitions is mostly Δ_1 and the final state for primary cone emission is also Δ_1 (again without electron spin), transitions from these heavy- and light-hole bands are forbidden in first order. However, the experimental geometry allows for small but nonzero electric-field components parallel to the sample surface, giving rise to dipole operators with Δ_3 and Δ_4 symmetry. This component accounts for the weak emission from the two upper valence bands.^{14,15}

From the normal emission spectra we determined the experimental valence band dispersions $E(\mathbf{k})$ which are shown in Fig. 3. The circles represent data points from the $\text{Cd}_{0.8}\text{Zn}_{0.2}\text{Te}$ spectra. The k vectors were obtained by using free-electron final-state bands. The solid lines are a polynomial fit to the data, and are primarily used to

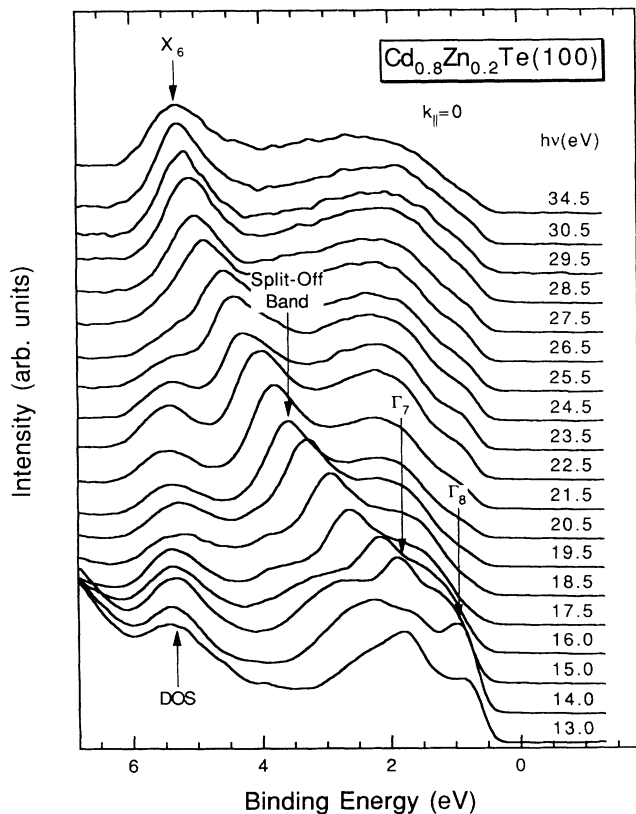


FIG. 2. Normal-emission valence-band spectra of $\text{Cd}_{0.8}\text{Zn}_{0.2}\text{Te}(100)$ measured in the photon energy range $h\nu = 13.0$ to 34.5 eV. The strongly dispersive feature is emission from the split-off band.

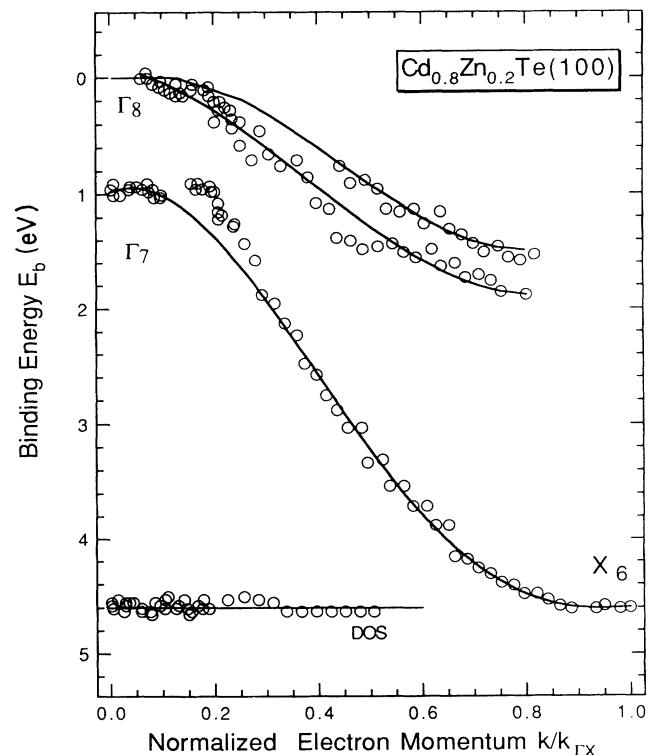


FIG. 3. Experimental valence band dispersion $E(k)$ for $\text{Cd}_{0.8}\text{Zn}_{0.2}\text{Te}(100)$.

guide the eye. As previously noted, the emission from the upper two valence bands is relatively weak, and as a result of that, the experimental data show a slightly higher uncertainty in this energy region than the data from the split-off band, which has considerably stronger photoemission features.

The kink in the data of the split-off band at $k/k_{\Gamma X} \sim 0.2$ is an artifact originating from shortcomings of the free-electron final-state-band conduction band near the Γ point. A more sophisticated final-state band model which would take the splitting of bands at the Brillouin-zone boundary into account, would place these transitions closer toward the Γ point. However, for the purpose of the present paper, the approximation of free-electron final-state bands is adequate and does not conflict with our interpretation. The effect of gaps in the final-state bands has been discussed in more detail elsewhere.¹⁵

We would now like to focus attention on the spin-orbit splitting $\Delta_{s.o.} = \Gamma_8 - \Gamma_7$ and the bandwidths $\Omega_{s.o.} = \Gamma_7 - X_6$ of the split-off band. Table I summarizes the theoretical and experimental values of $\Delta_{s.o.}$ and $\Omega_{s.o.}$ for CdTe, ZnTe, and $\text{Cd}_{0.8}\text{Zn}_{0.2}$. As one can see from Table I the experimental and theoretical spin-orbit splittings agree fairly well while the experimental X_6 -critical point energies are ~ 0.5 eV smaller than the calculated values, a fact which seems to be generally true for zinc-blende semiconductors. In the following estimation of $\Omega_{s.o.}(\text{Cd}_{0.8}\text{Zn}_{0.2}\text{Te})$, we have used the theoretical $\Omega_{s.o.}$ values for CdTe and ZnTe.²³

Figure 4 gives a closer look of the dispersion of the split-off band in $\text{Cd}_{0.8}\text{Zn}_{0.2}\text{Te}$ towards the X point. When comparing to CdTe which is shown in Fig. 4 as crosses, one may observe a 0.21-eV increase in binding energy of the X_6 point in $\text{Cd}_{0.8}\text{Zn}_{0.2}\text{Te}$ emission. Considering the ~ 0.04 -eV difference between the $\Delta_{s.o.}$, we determine an increase in $\Omega_{s.o.}$ of ~ 0.25 eV between $\text{Cd}_{0.8}\text{Zn}_{0.2}\text{Te}$ and CdTe.

One may rearrange the expression for $P(x)$ to read

TABLE I. Theoretical (theor.) and experimental (expt.) values of the spin-orbit splitting $\Delta_{s.o.} = \Gamma_8 - \Gamma_6$, X_6 critical point energies, and the bandwidth $\Omega_{s.o.} = \Gamma_7 - X_6$. The reference energy is the valence-band maximum with $E(\Gamma_8) = 0$. All energies are given in eV.

Material	Method	$\Delta_{s.o.}$	$\Gamma_8 - X_6$	$\Omega_{s.o.}$
CdTe	theor. ^a	0.89	5.05	4.16
	expt. ^b	0.95	4.40	3.45
ZnTe	theor. ^c	0.93	5.56	4.61
	expt. ^d	0.91	5.10	4.19
$\text{Cd}_{0.8}\text{Zn}_{0.2}\text{Te}$	expt. ^e	0.91	4.61	3.70

^aReference 19.

^bReference 20.

^cReference 21.

^dReference 22.

^eThis work.

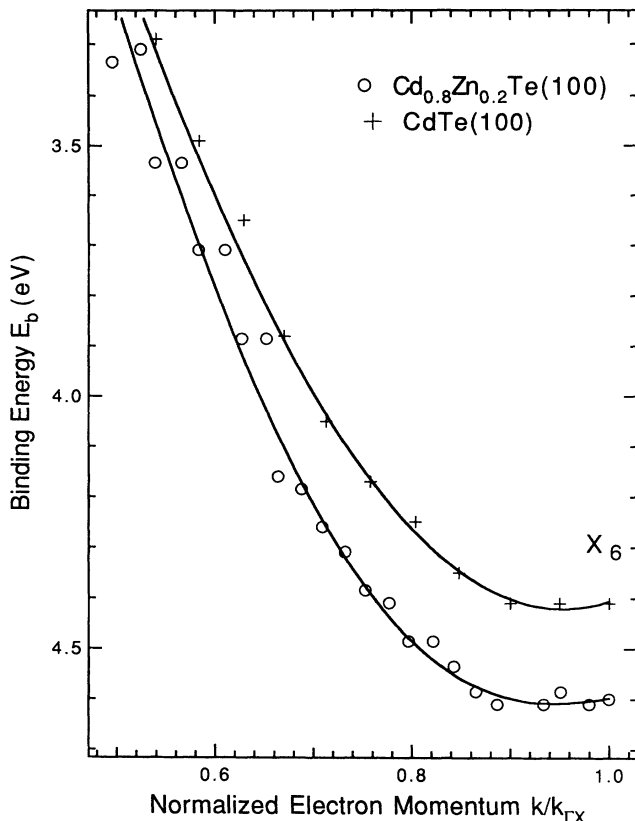


FIG. 4. Comparison of the experimental dispersion of the split-off band in $\text{Cd}_{0.8}\text{Zn}_{0.2}\text{Te}(100)$ and $\text{CdTe}(100)$ near the X point.

$$P(x) - P_{AC} = (P_{BC} - P_{AC})x + b_p x(1-x),$$

where now only differences enter into the equation. Using the experimental values from Table I and applying Vegard's rule ($b_p = 0$), one obtains 0.15 eV as the expected difference between the alloy and CdTe split-off-band width.²³ Vegard's rule underestimates the observed increase in bandwidth $\Omega_{s.o.} = 0.25$ eV by almost a factor of 2. Even though the absolute difference between the prediction of Vegard's rule and our measurement is relatively small it is outside the experimental uncertainty of ± 0.02 eV. Using the experimentally determined difference $\Omega_{s.o.}(\text{Cd}_{0.8}\text{Zn}_{0.2}\text{Te}) - \Omega_{s.o.}(\text{CdTe}) = 0.25$ eV, one may estimate the bowing parameter $b_p = 0.65 \pm 0.25$ eV.

Figure 5 shows the calculated concentration dependence of the bandwidth assuming a bowing parameter of $b_p = 0.65$ eV. The data point is the experimental value for $\text{Cd}_{0.8}\text{Zn}_{0.2}\text{Te}$, and the CdTe and ZnTe end points are taken from experiment.^{20,24,25} Several studies in the past decade show that, for instance, the fundamental band gap frequently has larger bowing parameters so that the alloy band gap may exceed the values of the constituent materials at certain concentrations.^{4,5,7,26} Recent results on $\text{ZnSe}_{1-x}\text{Te}_x$ alloys indicate that the optical band gap overshoots in the range $0.3 < x < 1.0$.⁹ Studies that have

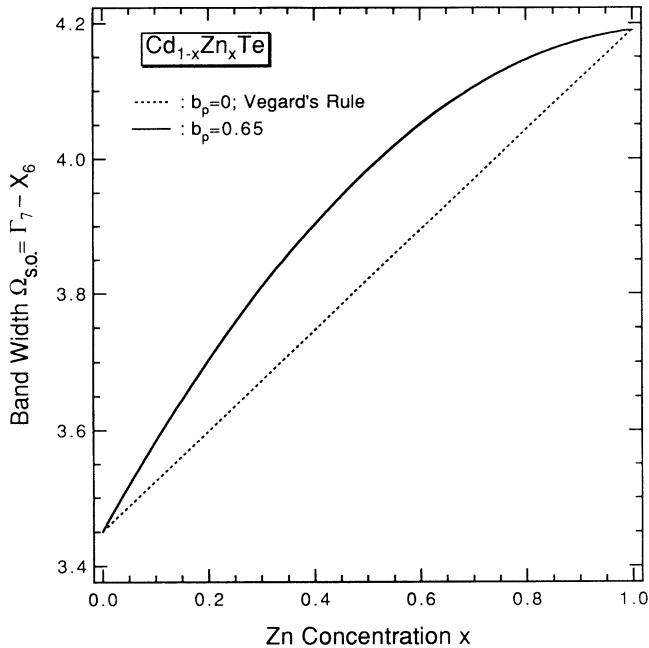


FIG. 5. Calculated split-off-band width in $\text{Cd}_{1-x}\text{Zn}_x\text{Te}$ as a function of the Zn concentration of x . The solid line represents a prediction of the VCA with a bowing parameter $b_p=0.65$ eV. The bandwidth variation is based on the experimental values of the alloy and the constituent components as listed in Table I. The dashed line shows the linear variation of the bandwidth assuming Vegard's rule.

examined the bowing parameter for optical band gap of $\text{Hg}_{1-x}\text{Cd}_x\text{Te}$ (size matched) and $\text{Hg}_{1-x}\text{Zn}_x\text{Te}$ (size mismatched) alloys have suggested that bowing is pronounced for materials which are size mismatched.^{7,26,27} These findings indicate our estimation of a bowing parameter b_p which forces the split-off bandwidth to overshoot in the size mismatched $\text{Cd}_{1-x}\text{Zn}_x\text{Te}$ system is not unreasonable.

A large bowing parameter indirectly implies a high degree of alloy disorder. *A priori* one might expect that disorder leads to prominent splittings or broadening in energy levels. For instance, Wei and Zunger showed for $\text{Cd}_{0.5}\text{Zn}_{0.5}\text{Te}$ that relaxation of the individual Cd and Zn bonds from the VCA average position results in a ~ 0.2 -eV splitting in the split-off band near the X_6 point.⁸ This splitting is not present in unrelaxed $\text{Cd}_{0.5}\text{Zn}_{0.5}\text{Te}$ where only the chemical mismatch between Cd and Zn is considered. A careful comparison of our CdTe and $\text{Cd}_{0.8}\text{Zn}_{0.2}\text{Te}$ spectra in this study shows that there is no real evidence for such changes. The reason we do not observe a splitting may be that the splitting is below our experimental resolution. The relatively small Zn concentration ($x=0.2$) in our sample may also be of a disadvantage to observe the predicted disorder induced splittings.

One expects to see larger effects due to the chemical and size mismatch between the Cd and Zn atoms in the more localized metal d states, however. While the upper three valence-band states are extended in character, the

more localized Cd $4d$ and Zn $3d$ states see potentials which resemble those of the pure CdTe and ZnTe crystals. States which are centered on the Te atoms, on the other hand, are affected by the varying alloy environment, i.e., a tetrahedral coordination $\text{Cd}_{4-x}\text{Zn}_x$.

The binding energy of the $4d$ states in CdTe is about 0.8 eV higher than the Zn $3d$ states in ZnTe.^{22,24,28} Figure 6(a) shows the spectrum of the metal d states of the $\text{Cd}_{0.8}\text{Zn}_{0.2}\text{Te}$ alloy measured at $h\nu=24$ eV. The main peak at ~ 10 eV is due to the Cd $4d$ emission while the shoulder at ~ 9.2 -eV binding energy can be assigned to the Zn $3d$ states. The solid line was obtained by fitting two spin-orbit-split doublets and a background (due to inelastic electron scattering) to the experimental data. The fitted spin-orbit splitting is $\Delta_{s.o.}=0.69$ eV between the $4d_{3/2}$ and $4d_{5/2}$ states. For the Zn $3d$ components, we determined a spin-orbit splitting of 0.68 eV.

The intensity of the Zn emission is $\sim 13\%$ of the total intensity. Incorporating the atomic photoemission cross sections which are $\sigma(\text{Cd } 4d) \sim 10$ Mb and $\sigma(\text{Zn } 4d) \sim 6$ Mb at $h\nu=24$ eV, we conclude that the measured Zn intensity agrees fairly well with the nominal Zn concentra-

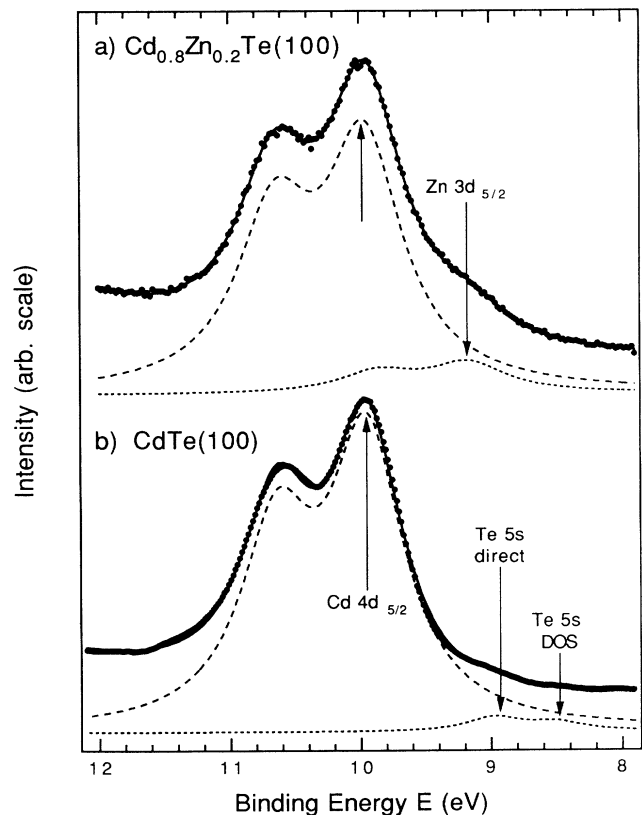


FIG. 6. (a) Photoemission spectra of Cd $4d$ - and Zn $3d$ -derived states. The appearance of a shoulder on the lower binding energy side which is related to the Zn $3d$ emission indicates the limitations of the VCA. (b) The CdTe(100) spectrum also shows a shoulder which is weaker and shifted further towards lower binding energy. This structure is related to direct transitions from the Te $5s$ band.

tion in the sample.²⁹ For comparison, we also show the normal emission spectrum of the CdTe(100) surface in Fig. 6(b). The CdTe spectrum has also a small shoulder, but its energy position is 0.3 eV lower and less intense than the Zn 3*d* feature in Fig. 6(a). Moreover, the CdTe shoulder which is associated with transitions from the Te 5*s*-derived band disperses with photon energy, while the Zn 3*d* feature is nondispersive.²⁸

In the VCA approximation, there should only be one band which would be a composite of the Cd 4*d*, Zn 3*d*, and Te 5*s* states. However, we observe a strong emission which stems from the Cd 4*d* states and a weaker feature at ~1 eV lower binding energy from the Zn 3*d* state. The structural alloy model by Wei and Zunger predicts a doublet structure for this band with a splitting of ~1.25 eV between the predominantly Cd 4*d* and Zn 3*d* components.⁸

When viewed as core levels, the presence of two distinct features is not too surprising. In fact, Marbeuf *et al.* observe distinct Zn 3*d* and Hg 5*d* emissions from Hg_{1-x}Zn_xTe alloys.^{26,27} Wall *et al.* also reported distinct *d*-state emission from other II-VI binary alloys.^{30,31} However, the proximity of the *d* states to the *s* and *p* states which comprise the valence bands makes them non-negligible in band-structure calculations.³² Investigations on CdTe(110) have shown that the Cd 4*d* level mixes with the Te 5*s* states and as a result of that show a small dispersion.²⁸ To this extent, one would have to incorporate the chemical mismatch between Cd and Zn atoms. The observed splitting into two separate *d* bands exemplifies a fundamental limitation of the VCA for semiconducting compound alloys.

IV. CONCLUSIONS

The VCA works well for the delocalized *sp* states which comprise the top three valence bands of the

Cd_{1-x}Zn_xTe alloy. The model, however, fails for the more localized shallow metal *d* states, where chemical as well as size mismatch between the Cd and Zn atoms cause a noticeable splitting between the 3*d* and 4*d* states. The observed splitting is outside the scope of the VCA because the model would replace the individual Cd and Zn atoms by a new "average" atom.

It is expected that the increased localization of the valence electron in the split-off band around the *X* point also causes a small splitting at the zone boundary, although the present data do not substantiate this possibility.⁸ With sufficient energy resolution, one may observe a splitting or at least a broadening of the photoemission features from this region of the Brillouin zone.

The bowing parameter $b_p = 0.65$ eV, which we determined from the width of the split-off band, implies that nonlinear effects are significant the electronic band structure of Cd_{1-x}Zn_xTe alloys. Since the Cd and Zn atoms are chemically as well as size mismatched, a large degree of statistical disorder makes our estimation of the increased split-off band width plausible. To evaluate the disorder effect on the bowing parameter further, we plan to study Cd_{1-x}Zn_xTe alloys for a concentration near $x = 0.5$ where the deviation from linearity will be most pronounced. Since Cd_{1-x}Zn_xTe single crystals of arbitrary Zn concentrations are not commercially available we first need to study the molecular-beam epitaxy growth of thin strain free alloy films.

ACKNOWLEDGMENTS

The authors would like to thank the staff of the Synchrotron Radiation Center for technical support. The operation of the Synchrotron Radiation Center is funded by the National Science Foundation.

¹L. Vegard, *Z. Phys.* **5**, 17 (1921).

²L. Nordheim, *Ann. Phys. (Leipzig)* **9**, 607 (1931).

³J. A. Van Vechten and T. K. Bergstresser, *Phys. Rev. B* **1**, 3351 (1970).

⁴D. J. Chadi, *Phys. Rev. B* **16**, 790 (1977).

⁵P. Parayanthal and F. H. Pollak, *Phys. Rev. B* **28**, 3632 (1983).

⁶J. E. Bernard and A. Zunger, *Phys. Rev. B* **36**, 3199 (1987).

⁷J. Camassel, J. P. Laurenti, A. Bouhemadou, R. Legros, A. Lussou, and B. Toulouse, *Phys. Rev. B* **38**, 3948 (1988).

⁸S.-H. Wei and A. Zunger, *Phys. Rev. B* **43**, 1662 (1991), and references therein.

⁹F. S. Turco-Sandroff, R. E. Nahory, M. J. S. P. Brazil, R. J. Martin, and H. L. Gilchrist, *J. Cryst. Growth* **111**, 762 (1990). *Appl. Phys. Lett.* **58**, 1611 (1991).

¹⁰S. Fujita, S. Hayashi, M. Funato, and T. Yoshie, *J. Cryst. Growth* **107**, 674 (1991).

¹¹P. Kashyap, M. Jain, and H. K. Sehgal, *Infrared Phys.* **30**, 285 (1990).

¹²W. E. Spicer, J. A. Silberman, J. Morgen, I. Lindau, J. A. Wilson, An-Ban Chen, and A. Sher, *Phys. Rev. Lett.* **49**, 948 (1982).

¹³K. L. Tsang, J. E. Rowe, T. A. Callcott, and R. A. Logan, *Phys. Rev. B* **38**, 13277 (1988).

¹⁴W. Eberhardt and F. J. Himpsel, *Phys. Rev. B* **21**, 5572 (1980).

¹⁵D. W. Niles and H. Höchst, *J. Vac. Sci. Technol. A* **10**, 1526 (1992).

¹⁶G. P. Williams, F. Cerrina, G. J. Lapeyre, J. R. Anderson, R. J. Smith, and J. Hermanson, *Phys. Rev. B* **34**, 5548 (1986).

¹⁷E. W. Plummer and W. Eberhardt, *Adv. Chem. Phys.* **49**, 533 (1982).

¹⁸R. Brigans, in *Angular Resolved Photoemission*, edited by S. D. Kevan (Elsevier, New York, in press).

¹⁹J. R. Chelikowsky and M. L. Cohen, *Phys. Rev. B* **12**, 556 (1976).

²⁰D. W. Niles and H. Höchst, *Phys. Rev. B* **43**, 1492 (1991).

²¹D. Bertho, D. Boiron, A. Simon, C. Jouanin, and C. Priester, *Phys. Rev. B* **44**, 6118 (1991).

²²L. Ley, A. Pollak, F. R. McFreely, S. P. Kowalczyk, and D. A. Shirley, *Phys. Rev. B* **9**, 600 (1974).

²³We have chosen to use consistent experimental rather than theoretical values for $\Omega_{s.o.}(\text{CdTe})$ and $\Omega_{s.o.}(\text{ZnTe})$ to estimate an expected change between CdTe and Cd_{0.8}Zn_{0.2}Te. Using

- theoretical values does not change any of the conclusions about bowing in $\Omega_{s,o}$.
- ²⁴E. Colavita, M. A. Engelhardt, and H. Höchst (unpublished).
- ²⁵D. Richardson, *J. Phys. C* **5**, L27 (1972).
- ²⁶A. Marbeuf, D. Ballataud, R. Triboulet, H. Dexpert, P. Lagarde, and Y. Marfaing, *J. Phys. Chem. Solids* **50**, 975 (1989).
- ²⁷A. Marbeuf, D. Ballataud, R. Triboulet, and Y. Marfaing, *J. Crys. Growth* **101**, 608 (1990).
- ²⁸H. Höchst, D. W. Niles, and I. Hernández-Calderón, *Phys. Rev. B* **40**, 8370 (1989).
- ²⁹J. J. Yeh and I. Landau, *At. Data Nucl. Data Tables* **32**, 1 (1985).
- ³⁰A. Wall, C. Caprile, A. Franciosi, R. Reifenberger, and U. Debska, *J. Vac. Sci. Technol. A* **4**, 818 (1986).
- ³¹A. Wall, A. Franciosi, Y. Gao, J. H. Weaver, M.-H. Tsai, J. D. Dow, and R. V. Kasowski, *J. Vac. Sci. Technol. A* **7**, 656 (1989).
- ³²S.-H. Wei and A. Zunger, *J. Vac. Sci. Technol. A* **6**, 2597 (1988).